

Solvent Effect on Structural Change of Poly(vinyl alcohol) Physical Gels

PO-DA HONG, JEAN-HONG CHEN, HUEI-LI WU

Graduate School of Textile and Polymer Engineering, National Taiwan University of Science and Technology, Taipei 10672, Taiwan, Republic of China

Received 10 November 1997; accepted 5 January 1998

ABSTRACT: In this study, the relationship between the polymer–solvent interaction and the network structure of poly(vinyl alcohol) (PVA) gels prepared with organic solvents such as *N*-methylpyrrolidone (NMP) and ethylene glycol (EG) are investigated. The values of the intrinsic viscosity $[\eta]$ and Huggins constant k' of dilute PVA solutions indicate that the attractive interaction between PVA and NMP is higher than that between PVA and EG. The X-ray result shows that PVA–EG gels have a (101) diffraction peak of PVA crystal that appeared at about $2\theta = 19^\circ$, while PVA–NMP gels only show a broad amorphous scattering peak. On the other hand, Fourier transform infrared results of PVA/EG gels also clearly show an intense peak at 1141 cm^{-1} due to the crystalline absorption. The results of H^1 pulsed nuclear magnetic resonance show that the spin–spin relaxation time, T_2^s and T_2^l , respectively, related to the polymer-rich and polymer-poor components decrease, and the fractional amount of the polymer-rich component, f^s , increases, while that of the polymer-poor component, f^l , decreases with an increase in the concentration of polymer. At a given concentration, the value of f^s in the PVA–EG gel is larger than that in the PVA–NMP one. These facts indicate that the crystallinity in the PVA–EG gel is higher than that in the PVA–NMP gel, implying that the aggregation of PVA chains is much easier in the poor solvent, EG, than in the good solvent, NMP. The structural change with aging time in the PVA–EG gel is very remarkable because of the significant syneresis, indicating that the opaque PVA–EG gel with higher crystallinity has a comparatively heterogeneous and unstable network structure than the PVA–NMP gel does. © 1998 John Wiley & Sons, Inc. *J Appl Polym Sci* 69: 2477–2486, 1998

Key words: poly(vinyl alcohol); crystallinity; gelation; phase separation

INTRODUCTION

Thermoreversible physical gels constitute three-dimensional networks whose junction points consist of physical bonds between polymer chains, that may generally give either a turbid crystalline gel or a transparent gel. Poly(vinyl alcohol)

(PVA) is well known as a crystalline polymer, and it has been suggested that the crystallization necessarily follows gelation in the semi-dilute solutions prepared from various solvents.^{1–11} PVA physical gels are believed to consist of crystalline and amorphous regions. The crystalline region consists of junction points that are the aggregation of ordered polymer sequences, while the amorphous region consists of long flexible chains connecting between junction points.^{12–13} Studies on PVA gels attract many interests because the relationship between the aggregation behavior of polymer chains and physical properties of gels is

Correspondence to: P.-D. Hong.

Contract grant sponsor: National Science Council of the Republic of China; contract number: NSC-86-2216-E011-008.

Journal of Applied Polymer Science, Vol. 69, 2477–2486 (1998)

© 1998 John Wiley & Sons, Inc.

CCC 0021-8995/98/122477-10

very complicated. Besides, the nature and structure of junction points are so complex that there are still subjects of some controversy.

It is well known that the PVA solutions can form gels with the various kinds of solvents, such as *N*-methyl-2-pyrrolidone (NMP), ethylene glycol (EG), dimethyl sulfoxide (DMSO), and mixtures of these solvents. Ohkura et al.^{3,4} have reported that PVA gels with higher elasticity prepared from DMSO–water-mixed solvents at below -20°C are transparent because the gelation rate is much faster than that of the phase separation. On the other hand, Klenina et al.¹⁴ pointed out that the PVA aqueous solution exhibited only an amorphous separation. Watase and Nishinari¹⁵ found that a smaller and broader endothermic peak at about 45°C and a sharper endothermic peak at 110°C are considered to be respectively attributed to the disentanglement of polymer chains and the gel melting from the DSC results of PVA–DMSO– H_2O gels. Our previous study¹ indicated that the drawability of dried PVA gel film is strongly affected by the structure of wet gel; that is, the gel with a more homogeneous structure exhibits higher drawability. These results, as mentioned above, mean that the differences in physical properties must be related to the structural changes of the gels. Generally, physical properties of physical polymer gels are considered to be dominated by the aggregation degree and the molecular mobility of polymer chains, which are related mainly to the degree of molecular interaction between polymer and solvent.

In this work, we first investigated the viscosity of PVA dilute solutions prepared with NMP and EG in order to determine the interaction degree between PVA and solvents. Then, the changes in the structure and properties of PVA gels with aging time were also studied. Finally, the interaction effect on the structural change of PVA gels was discussed through X-ray and Fourier transform infrared (FTIR) analyzes. Besides, the degree of chain aggregation and the crystallinity of gels were investigated using the pulsed nuclear magnetic resonance (NMR) analysis.

EXPERIMENTAL

PVA powder ($M_w = 155000$; Aldrich Chem. Co., USA) with high degrees of hydrolysis (about 99.8%) was used in this work. The solvents, NMP

and EG, were analytical grade and purified by distillation before using.

The homogeneous PVA solutions with various concentrations of PVA were obtained by heating at $120\text{--}130^{\circ}\text{C}$ for 2 h and then cooled to room temperature to form gels. A “test-tube upside-down” method for determining the gel melting point, T_m^G , of PVA gel prepared from different conditions of the gelation. The test tube with gel was kept upside down in a thermostat oven at heating rate of $0.5^{\circ}\text{C min}^{-1}$ to let the gel in test tube heat evenly. The temperature at which the gel began to flow was defined as the T_m^G of gel.

Determinations of the viscosity of dilute PVA solutions were carried out with an Ubbelohde viscometer immersed in a thermostatic water bath held at $30 \pm 0.5^{\circ}\text{C}$. The intrinsic viscosity, $[\eta]$, is obtained using the Huggins equation, as follows¹⁶:

$$(t - t_0/t_0)/C = (\eta_{sp}/C) = [\eta] + k'[\eta]^2C \quad (1)$$

where t is the time of flow of the dilute solution, t_0 is the time of flow of the pure solvent, C is the concentration of polymer, η_{sp} is the specific viscosity, and k' is the Huggins constant.

The infrared spectra were measured by using a Digilab Division BIO-RAD spc-3200 FTIR equipment. The transmittance peaks at 1141 and 1095 cm^{-1} were assigned to the crystalline and the amorphous sequences, respectively.^{17,18} The transmittance ratio of $1141/1095\text{ cm}^{-1}$ is the regulativity index of PVA gels.

The wide-angle X-ray diffraction (WAXD) photographs were taken by a flat camera with Ni-filtered $\text{Cu-K}\alpha$ radiation from a Rigaku XG working at 35 kV and 20 mA at the exposure time of 2 h. WAXD intensity curves of the gels were measured with a graphite-monochromatized $\text{Cu-K}\alpha$ radiation generated at 50 kV and 180 mA in a Rigaku D/max diffractometer at scanning speed of $2\theta = 1^{\circ}\text{ min}^{-1}$.

^1H pulsed NMR measurements were performed with an MARAN-20 pulsed NMR spectrometer operating at a fixed frequency of 20 MHz at 30°C . The recovery time of the spectrometer following a sequence of pulse was $13\ \mu\text{s}$. The spin–spin relaxation time, T_2 , measurements were carried out using the solid echo¹⁹ [free induction decay (FID)] pulsed sequence ($90^{\circ}_x\tau 90^{\circ}_y$) ($\text{P}90^{\circ} = 2.8\ \mu\text{s}$) available for short T_2 sample, for example, crystalline domains in gel systems, to avoid the effect of the dead time after the pulse, and Carr–Purcell–Meiboom–Gill (CPMG)²⁰ pulsed se-

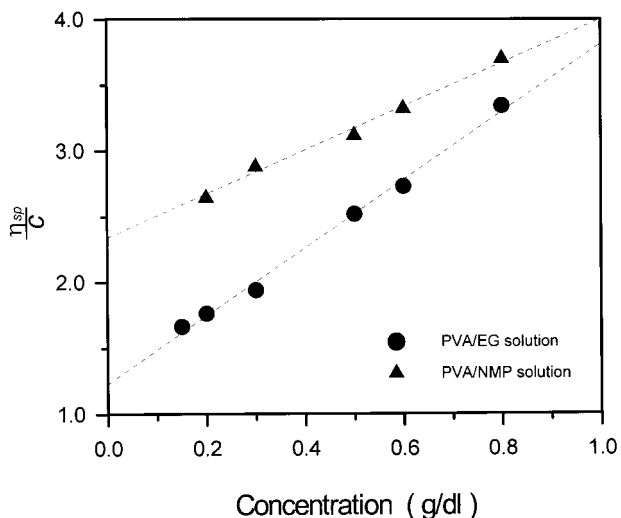


Figure 1 Plots of η_{sp}/C as a function of C for PVA dilute solutions.

quence $[90^{\circ}_x \tau (180^{\circ}_y 2\tau)_n]$ ($P90^{\circ} = 2.8 \mu\text{s}$, $P180^{\circ} = 5.6 \mu\text{s}$, and $n = 4000$) available for a long T_2 sample, for example, the wet gel system, to eliminate the effect of heterogeneity in the static magnetic field.

RESULTS AND DISCUSSION

Figure 1 shows the η_{sp}/C value for PVA dilute solutions as a function of C . From the linear relationship in Figure 1, the Huggins constant k' and the intrinsic viscosity $[\eta]$ could be estimated using eq. (1). A solution with a lower value of k' (less than 0.4) and a higher value of $[\eta]$ is generally considered to be a good solvent, that is, with higher solubility and strongly attractive interaction between polymer and solvent. The calculated result shows that the value of k' for PVA–EG solution is about 1.53, while that for PVA–NMP solution is about 0.23. On the other hand, the $[\eta]$ of PVA–NMP solution (2.34 dL/g) is larger than that of PVA–EG solution (1.28 dL/g). These facts indicate that the affinity to PVA for NMP is larger than that for EG; that is, the attractive interaction between polymer and solvent in PVA–NMP solution is higher than that in the PVA–EG solution. NMP has the doubly bound oxygen in the chemical structure, resulting in a strong electron donor or a good hydrogen acceptor. The high dipole moment ($4.09 \times 10^{-30}\text{C m}$) can be attributed to the partial double bond character of the carbonyl carbon–nitrogen bond. Patel et al.²¹ have

already studied the solubility of PVA–NMP solution in detail and reported that NMP is a better solvent for PVA than water and DMSO are. On the other hand, although the chemical structure of EG molecule is similar to that of PVA monomer because the linear structure makes the dipole moment ($2.28 \times 10^{-30}\text{C m}$) of EG lower. Andreyeva et al.⁹ have also pointed out that only the use of solvents, such as diols and triols, that is, the solvents with a chemical structure that is similar to that of PVA, has made it possible to form the single crystal from the dilute PVA solutions. This may mean that the crystallization in PVA solution of the poor solution takes place much easier.

Figure 2 shows the WAXD photographs of PVA–EG and PVA–NMP wet gels. Although a large part of the scattering intensity in the PVA gel contributed mainly to that of solvents, comparison of these 2 WAXD photographs show that a sharper diffraction ring due to the PVA crystal is clearly observed in the PVA–EG gel, indicating that the PVA–EG gel has a higher crystallinity than the PVA–NMP gel. In our previous study,¹ some general properties have been compared between PVA–NMP and PVA–EG gels. PVA–NMP gels having higher elasticity were transparent, while PVA–EG gels were opaque. From the X-ray diffraction (XRD) pattern and turbidity of PVA–EG gels results indicate that a number of crystallites formed in PVA–EG gels during the gelation, making the chain aggregation large enough to scatter visible light; this aggregation behavior may be the same as that proposed by Stoks et al.¹¹ On the other hand, the syneresis was very obvious within a few minutes in PVA–EG gels, while no noticeable syneresis occurred in PVA–NMP gels for several days, implying that the ag-

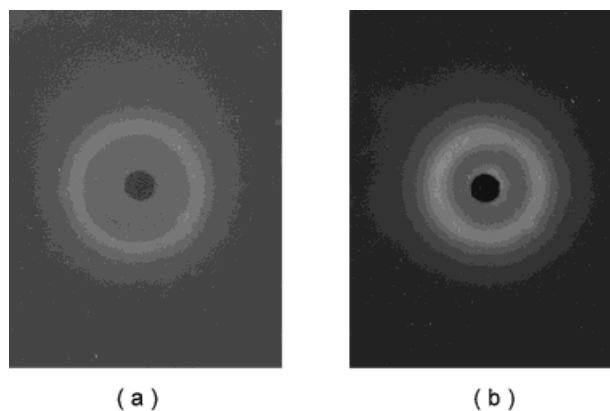


Figure 2 WAXD photographs of the PVA gels ($C = 8$ wt %): (a) PVA–EG gel; (b) PVA–NMP gel.

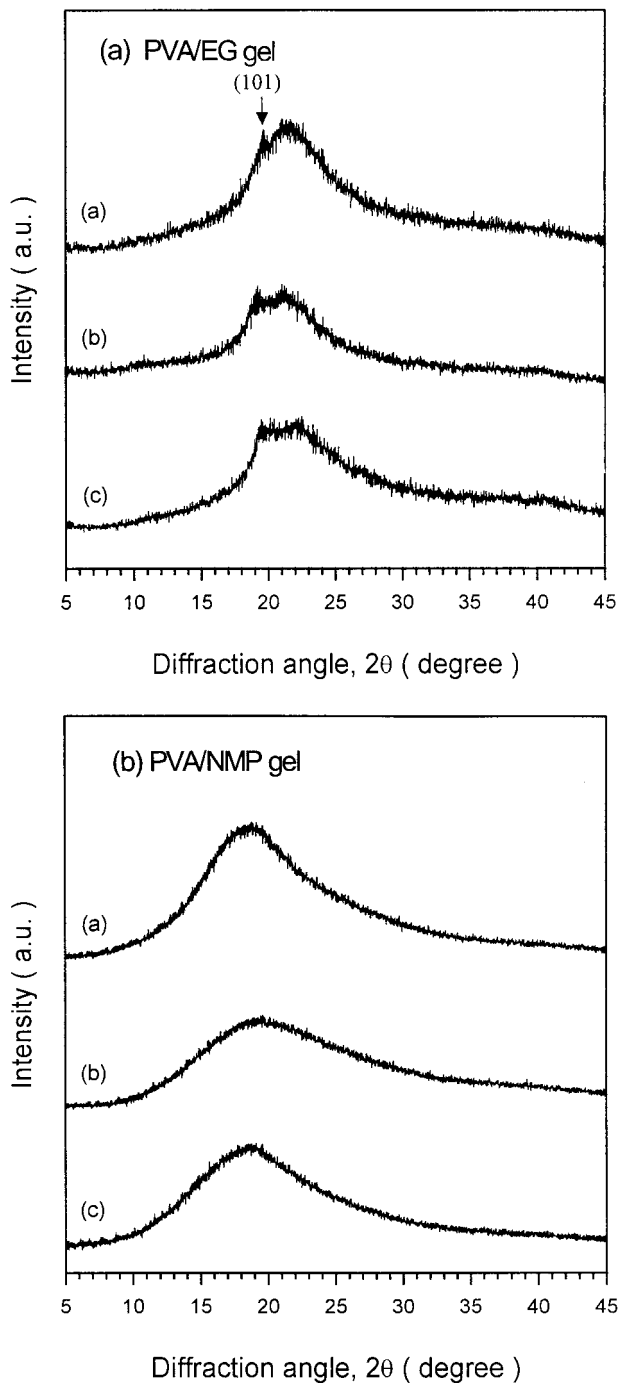


Figure 3 (a) WAXD intensity curves of the PVA-EG gels with various C : (a) 8, (b) 11, and (c) 15 wt %; (b) WAXD intensity curves of the PVA-NMP gels with various C : (a) 8, (b) 11, and (c) 15 wt %.

gregation of PVA chains takes place much easier in the solution of poor solvent.

Figure 3(a) and (b) show WAXD intensity curves of PVA-NMP and PVA-EG gels as a function of the concentration of PVA, respectively. Al-

though a large part of the intensity is the contribution of solvents, the (101) diffraction peak of PVA crystal clearly appears at about $2\theta = 19^\circ$ in PVA-EG gels but not in PVA-NMP gels. The intensity peak of the (101) diffraction becomes more obvious in PVA-EG gels, while PVA-NMP gels exhibit only an amorphous scattering peak as the concentration is increased. It should be noticeable that the (101) diffraction of PVA crystal is due to the intermolecular interference between PVA chains in the direction of the intermolecular hydrogen bonding. The increase in the intensity of the (101) diffraction corresponds to the increase in the number of PVA chains packing together, resulting in a larger size of the crystallite in PVA gels. A nearly amorphous or a lower crystalline PVA-NMP gel must have a homogeneous and thinner network structure, which is considered to be due to the higher polymer-solvent interaction, making the phase separation more difficult during the gelation.

Figure 4(a) and (b) shows the FTIR spectra of PVA-EG and PVA-NMP gels with various concentrations, respectively. The transmittance peaks at 1141 and 1095 cm^{-1} were assigned to the crystalline and the amorphous sequences, respectively. The transmittance ratio of 1141/1095 cm^{-1} is the regulativity index of PVA gel. The transmittance ratio of 1141/1095 cm^{-1} for PVA-EG gels is much larger than that for PVA-NMP gels. The intensity of the crystalline transmittance peak at 1141 cm^{-1} in PVA-EG gel increases remarkably with an increase in the concentration, while that in PVA-NMP gel is almost not detected, even at higher concentrations. This result of FTIR analysis is in a good agreement with that of X-ray analysis.

Figure 5 shows the melting temperature of gel, T_m^G , of PVA-NMP and PVA-EG gels as a function of the concentration, respectively. The result shows that the T_m^G increases remarkably in both PVA-NMP and PVA-EG gels with an increase in the concentration. On the other hand, the result also shows that the T_m^G of PVA-EG gel is higher than that of PVA-NMP gel at a given concentration. Eldridge and Ferry²² have provided a convenient relation, as shown in eq. (2) for calculating the enthalpy of formation of a mole of junction points, ΔH_m . The ΔH_m value is considered to be related with the average number of polymer chains held together in a junction point. Figure 6 shows the plot of $1/T_m^G$ versus $\ln C$, and exhibits a linear relationship in the experimental data.

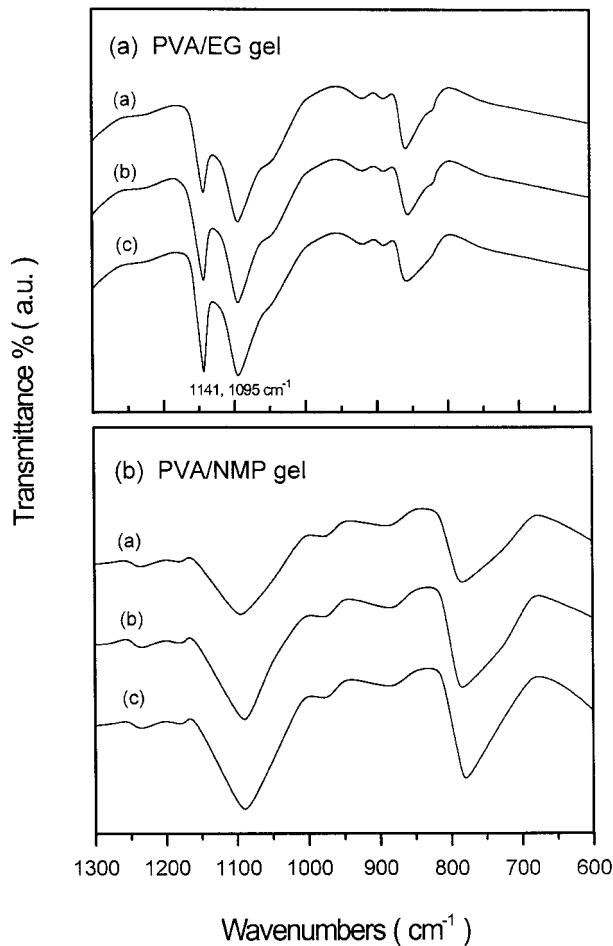


Figure 4 (a) FTIR spectra of the PVA–EG gels with various C : (a) 8, (b) 11, and (c) 15 wt %; (b) FTIR spectra of the PVA–NMP gels with various C : (a) 8, (b) 11, and (c) 15 wt %.

This means that the Ferry–Eldridge relation may apply to PVA gel system in this study.

$$\ln C = \text{Const} + \Delta H_m / RT_m^G \quad (2)$$

The ΔH_m values for PVA–EG and PVA–NMP gels can be obtained from the slope of the linear relationship in Figure 6 according to eq. (2). Then the ΔH_m values of PVA–EG and PVA–NMP gels obtained from Figure 6 are about 150 and 65 kJ/mol, respectively. The ΔH_m value obtained in this work for PVA–EG gel is close to that reported by Yamuaura et al.²³ They showed the ΔH_m values varied from 172 to 238 kJ/mol for PVA–EG gels prepared from the different PVAs. According to the result reported by Maeda et al.,²⁴ the enthalpy of the formation of hydrogen bonding between 2 PVA chains is about 21 kJ/mol. From the above

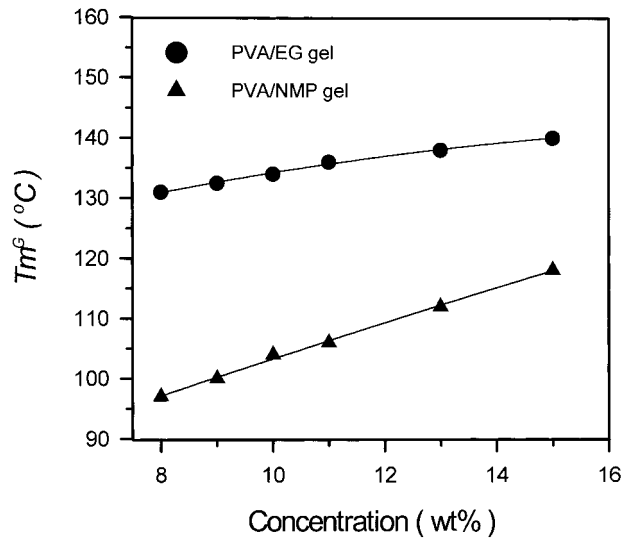


Figure 5 T_m^G of PVA gels as a function of C : (●) the PVA–EG gel; (▲) the PVA–NMP gel.

discussion, the crystallite size in PVA–EG gels consist of about 8 PVA chains packing together, while that in PVA–NMP gel only consists of about 3 PVA chains, although the effect of solvent quality on the thermal properties, such as the T_m^G of gels, could not be discussed through the Ferry–Eldridge relation. There is no doubt that the average size of the junction point in the PVA–EG gel is larger than that in the PVA–NMP gel, as is

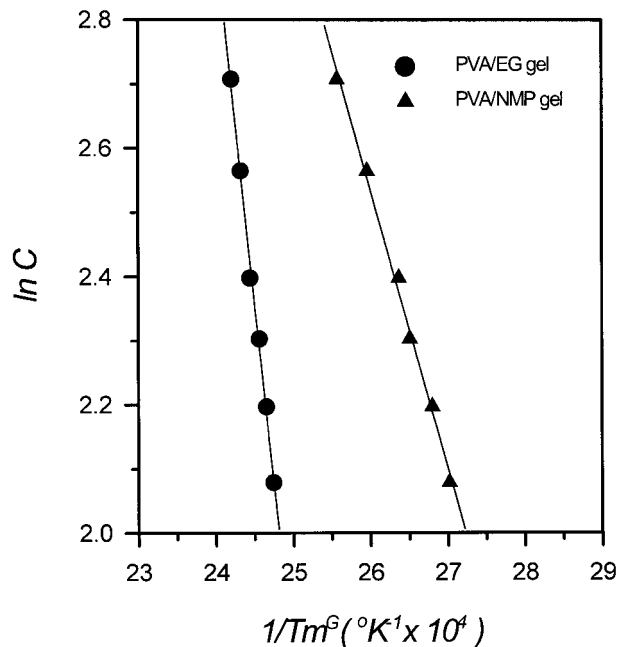


Figure 6 Plots of $1/T_m^G$ versus $\ln C$ of the PVA gels: (●) the PVA–EG gel; (▲) the PVA–NMP gel.

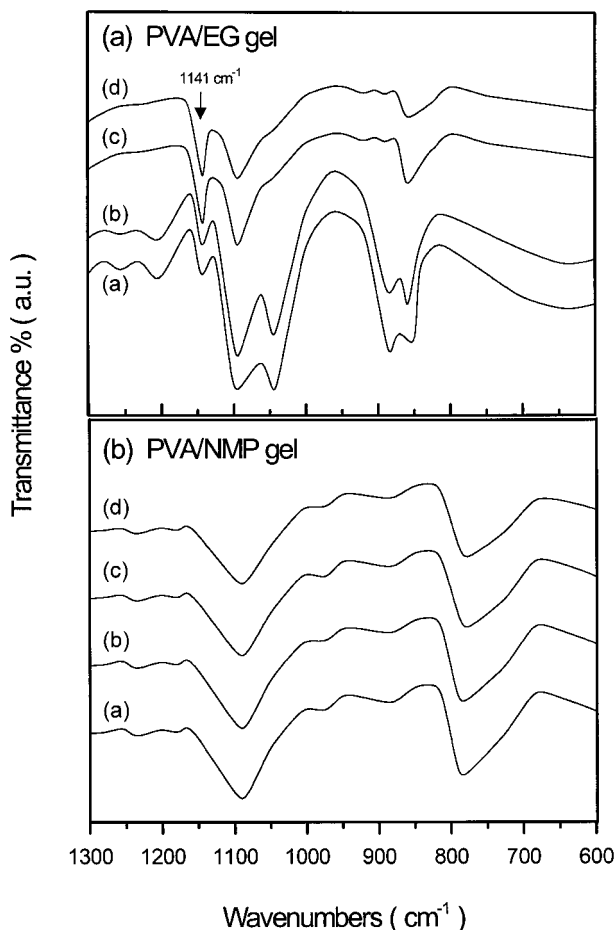


Figure 7 FTIR spectra of the PVA gels ($C = 8$ wt %) as a function of aging time: (a) fresh gel; (b) 4 h aging; (c) 1-day aging; (d) 4-day aging.

like the results in both WAXD and FTIR. These results let us consider that the gelation of PVA–NMP solution must occur before the phase separation because the PVA–NMP samples have no remarkable change in their transparent appearance during the gelation from the semi-dilute solution state. On the other hand, PVA–EG solutions first become turbid, and then the gelation occurs to form opaque gels. In other words, the phase separation takes place before the gelation.

The effect of aging time on the structural change and physical properties of PVA–DMSO–water gels has been investigated by Tanigami et al.²⁵ They pointed out that the enhancement of the gel modulus and the solvent exclusion could be attributed to phase separation crystallization in PVA–DMSO–water gels. Figure 7(a) and (b), respectively, show the FTIR spectra of PVA–EG and PVA–NMP gels as a function of the aging time. The intensities of transmittance peaks at

890 and 1045 cm^{-1} related to EG solvent decrease remarkably, while the intensity of PVA crystalline transmittance peak at 1141 cm^{-1} increases with an increase in aging time. On the other hand, there is no remarkable change in the FTIR spectra of PVA–NMP gels with an increase in aging time. The syneresis process is due to the volumetric shrinkage of gels accompanying solvent exclusion from gels. Therefore, the remarkable syneresis in PVA–EG gels indicates that the chain aggregation easily proceeds further during the aging process. The syneresis in PVA–EG gels caused by the phase separation must be a main reason for the increase of the crystallinity with the aging time. Ohkura et al.²⁶ showed that the UV transmission of the PVA–DMSO–water solution decreases with an increase in time at a given temperature. They also considered that the gel prepared at a lower temperature yields a phase separation in the network structure after gelation. It is reasonable that the strongly attractive interaction between PVA and NMP must produce the gels with a comparatively homogeneous and stable network structure.

It is well known that physical gel systems often exhibit a heterogeneous structure, which leads to the heterogeneity in chain mobility with a multi-exponential decay of transverse magnetization in pulsed NMR.^{27–29} Generally, the decaying signals of the transverse magnetization intensity, $M(t)$, could be expressed empirically, as in the following Weibull function^{30,31}:

$$M(t) = M_0 \exp[-(1/a)(t/T_2)^a] \quad (3)$$

where M_0 is a constant proportional to the total number of the nuclei with magnetic moment, T_2 is the spin–spin relaxation time, and t is decay time. The value of a is the shape parameter, $1 \leq a \leq 2$, which could express the characteristic of different component. For $a = 1$, the T_2 can be disposed to the mobile component, and for $a = 2$, the T_2 can be disposed to the immobile component in the material, respectively. The nonlinear least-square method, which fits the experimental data into the following equation, makes the analysis of the decaying process, as follows:

$$M(t) = M_{0A} \exp\left\{-\frac{1}{2} (t/T_{2A})^2\right\} + M_{0B} \exp(-t/T_{2B}) \quad (4)$$

where M_{0i} is the magnetic moment fraction of i th

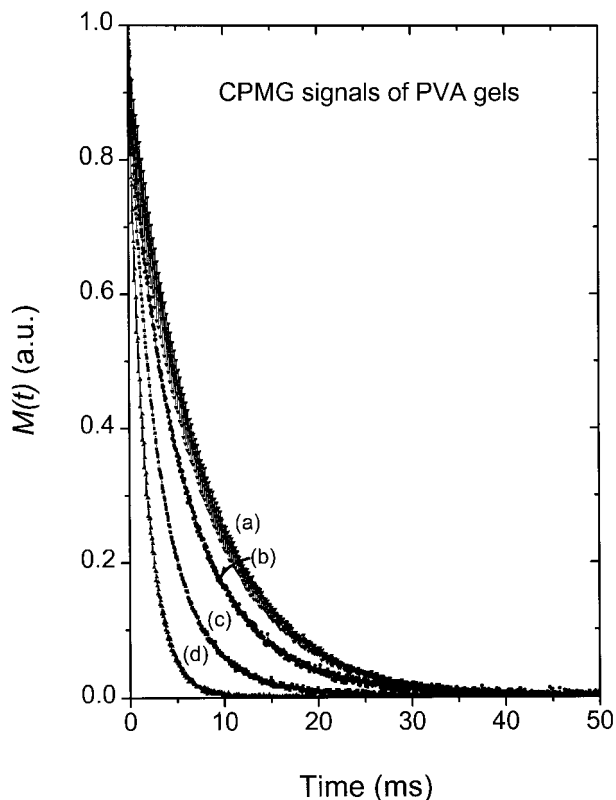


Figure 8 Decaying signals of CPMG for the PVA gels: (a) the PVA-NMP gel, $C = 8$ wt %; (b) the PVA-NMP gel, $C = 15$ wt %; (c) the PVA-EG gel, $C = 8$ wt %; (d) the PVA-EG gel, $C = 15$ wt %.

component, and T_{2i} is the spin-spin relaxation time of i th component. From this fitting procedure, we found that the CPMG decaying signals of PVA gels could be decomposed roughly into 2 components. The fast decaying signals are from the chain mobility in the immobile polymer-rich component related to the crystallite and the denser chain aggregation, and the slow decaying ones are from that in the mobile polymer-poor component related to the flexible chain connected between junction points and the free solvent molecules.

Figure 8 shows the CPMG decaying signals for various PVA gels. The CPMG decaying signals of all specimens are first decomposed roughly into 2 components using eq. (4) for calculating T_2 and the fractional amount f of each component. Figure 9(a) and (b), respectively, show the T_2 and f values of each component for PVA-NMP and PVA-EG gels as a function of the concentration. The f^l and f^s values are the fractional amount of long T_2 (T_2^l) and short T_2 (T_2^s) components, which are related to the polymer-poor and the polymer-rich

phases in gels, and the f value of each component is obtained from $f^s = [M_{0A}/M(t)] \times 100\%$ and $f^l = [M_{0B}/M(t)] \times 100\%$, respectively. The result shows that PVA-NMP samples have only a T_2^l

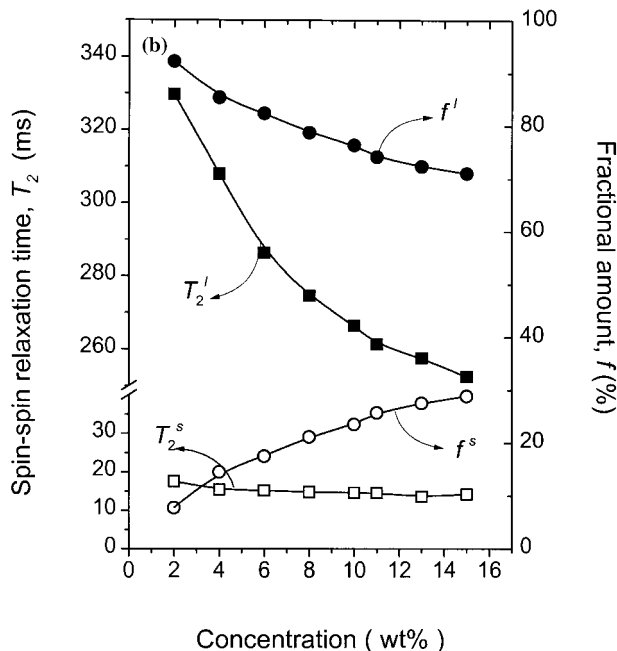
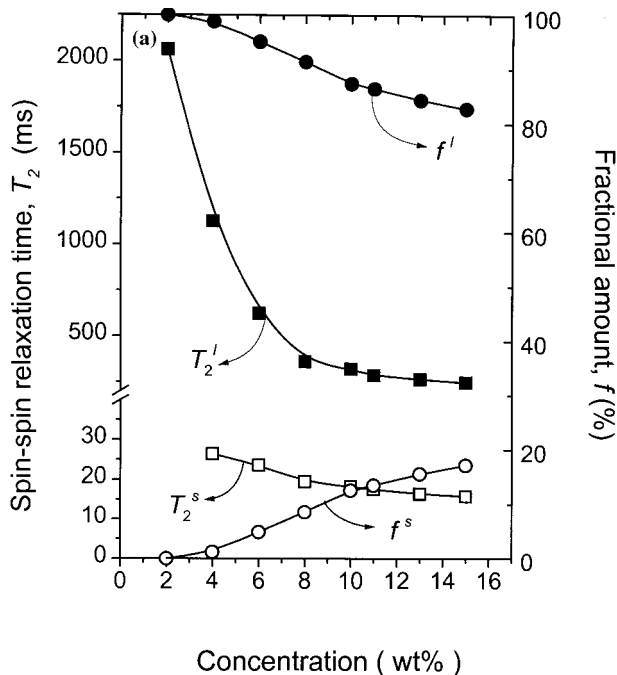


Figure 9 (a) Spin-spin relaxation time T_2 and fractional amount f of each component in the PVA-NMP gels as a function of C : (■) T_2^l ; (□) T_2^s ; (●) f^l ; (○) f^s . (b) Spin-spin relaxation time T_2 and fractional amount f of each component in the PVA-EG gels as a function of C : (■) T_2^l ; (□) T_2^s ; (●) f^l ; (○) f^s .

component below $C = 4$ wt %, while PVA–EG samples have already exhibited $2 T_2$, that is, the T_2^l and T_2^s components at $C = 2$ wt %, indicating that the critical gelation concentration of PVA–EG solution is lower than that of PVA–NMP solution.

Figure 9(a) also shows that the T_2^l value of PVA–NMP gel first decreases rapidly from about 2100 to 650 ms at the lower concentration range, from 2 to 6 wt %, and then slightly decreases from 650 to 250 ms at the higher concentration range. On the other hand, the T_2^s value only shows a small decrease from 27 to 15 ms with increasing concentration for PVA–NMP gels. The f^l value decreases, while the f^s value increases as the concentration is increased. Similar results, as shown in Figure 9(b), are obtained in PVA–EG gels, and the time scale of the T_2 value at lower concentration range is shorter than that for PVA–NMP gels. This may be not only due to the different chain mobility of the solvent molecules but also to the aggregation degree of polymer chains. Because the gelation of PVA–EG solution has already taken place gives rise to the reduction of polymer chain mobility, while that of PVA–NMP solution does not occur at the concentration below 4 wt %. It is reasonable that the increase in the degree of chain aggregation must give rise to reduce the chain mobility of polymer chains, resulting in a significant decrease of the T_2^l value from the semi-dilute solution or the sol states to the gel state. The main difference in the T_2^l value between these 2 gel systems is that, at a higher concentration range, the T_2^l value of PVA–EG gel is about 10 ms lower than that of PVA–NMP gel, indicating the polymer chains in the polymer-poor phase for PVA–NMP gel are more flexible than those for PVA–EG gel. This is considered to be due to the degree of chain aggregation, which must restrict the chain mobility between junction points. No remarkable change in the T_2^s value is considered due to the fact that the chain mobility is related to the polymer-rich phase of the gel network, which consists mainly of the denser chain entanglements and the crystallites. Therefore, the constrained chains within the polymer-rich phase may yield similar chain mobility with the same degree of the T_2^s value at this decaying time range, irrespective of the polymer concentration in the gel state.

From the above discussion, it is very clear that the aggregation degree of polymer chains in PVA–EG gels is larger than that in PVA–NMP gels because the polymer–solvent interaction in PVA–

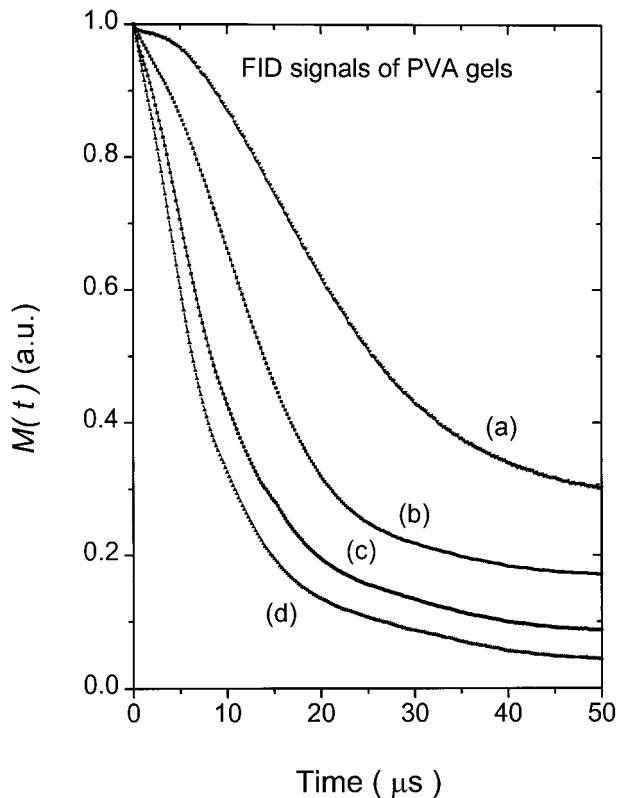


Figure 10 Decaying signals of FID for the PVA gels: (a) the PVA–NMP gel, $C = 8$ wt %; (b) the PVA–NMP gel, $C = 15$ wt %; (c) the PVA–EG gel, $C = 8$ wt %; (d) the PVA–EG gel, $C = 15$ wt %.

EG solution is lower than that in PVA–NMP solution. However, there is no direct evidence to indicate that the difference in the crystallinity of the polymer-rich phase between PVA–NMP and PVA–EG gels is shown in the results of the CPMG analysis at the longer decaying time range because the T_2^s and the f^s values of these 2 gels have no significant difference. Under this circumstance, the much shorter T_2 component related to the crystallites in the polymer-rich phase are separated from the free induction decay (FID) decaying signals at the shorter decaying time range using the solid echo technique. Figure 10 shows the decaying FID signals for gels. Shiga et al.²⁸ have reported that the T_2 value of the junction domains related to the PVA crystallite was about $10 \mu\text{s}$ in poly(vinyl alcohol)–poly(sodium acrylate) (PVA–PAA) gels. On the other hand, Fujimoto and Nishi³² also considered that the T_2 value of approximately $10 \mu\text{s}$ was contributed to the molecular motion in the crystal region from many pulsed NMR results for some crystalline polymers, such as Nylon 6, low-density polyethylene

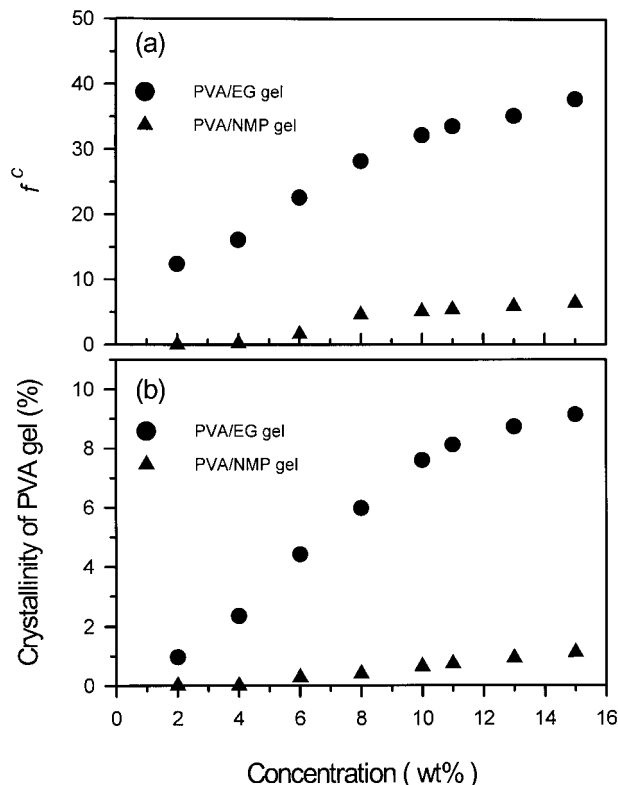


Figure 11 (a) Fractional amount of the crystallite f^c in the polymer-rich phase as a function of C . (b) Crystallinity of PVA gels as a function of C : (●) the PVA–EG gel; (▲) the PVA–NMP gel.

(LDPE), and high-density polyethylene (HDPE). Consequently, these results let us assume that the $T_2 = 10 \mu\text{s}$ component should be contributed to the junction points crystallites in the polymer-rich phase of PVA gels.

Figure 11(a) shows the fractional amount of the crystallite, f^c , in the polymer-rich phase, which is obtained from the separation of the $T_2 = 10 \mu\text{s}$ component in the FID decaying signals as a function of the concentration. Figure 11(b) shows the crystallinity of the PVA gels, which is obtained from the product of the f^s and f^c values, as shown in Figures 9 and 11(a). The crystallinity of the PVA–EG gel increases gradually from 1 to about 9%, while that of the PVA–NMP gel has no remarkable change with a very low value of approximately 1% as the concentration is increased. It should be noted that the f^s values of the PVA–NMP and PVA–EG gels, as shown in Figure 9, are in the range from 10 to 20%. The only 1% crystallinity in the PVA–NMP gel indicates that the primary part of the polymer-rich phase consists mainly of the denser chain entan-

gements. The quality of the polymer-rich phase is quite different between the PVA–NMP and PVA–EG gels. This phenomenon must be due to the different polymer–solvent interaction making the different gelation mechanism take place from the semi-dilute solution state. Generally, the polymer solution exhibits the liquid–liquid phase separation under cooling process. The liquid–liquid phase separation is usually related to the nucleation-controlled process and the spinodal decomposition. The gelation mechanism of the PVA–NMP system must be first induced by the spinodal decomposition and then followed by the slight crystallization within this region, resulting in a homogeneous and thinner network structure. On the contrary, the crystallization in the PVA–EG system must take place before the gelation because the poor solubility of the solvent used is more favorable to the intramolecular crystallization for forming a chain-folded crystallite during gelation and then results in the gel with opaque appearance and higher crystallinity. This consideration could be suggested by Stoks et al.¹¹ from the study on the PVA–EG gel through the thermal and X-ray analyses. They proposed a model for the gelation mechanism of the PVA–EG solution. The model indicated that the PVA–EG gel prepared at room temperature consists of some particle-like aggregation (polymer-rich phase) as physical crosslinks in which many crystallites are present. The crystallinity obtained from the pulsed NMR in this work for the PVA–EG gel may provide other evidence for this model.

CONCLUSION

In this study, the X-ray result shows that the PVA–EG gels have a (101) diffraction peak of PVA crystal appeared at about $2\theta = 19^\circ$, while the PVA–NMP gels only show an amorphous characteristic peak. The FTIR result of the PVA–EG gels also shows an intense peak at 1141 cm^{-1} due to the crystalline absorption. These results indicate that an opaque or a higher crystalline PVA–EG gel must have a thicker network structure, which is considered to be due to the lower polymer–solvent interaction, making the phase separation easier during the gelation. Due to a remarkable syneresis, the crystallinity of the PVA–EG gels increases with an increase in aging time, indicating that the gels from poor solvent exhibit an unstable network structure. The pulsed NMR result indicates that the gelation rate of the

PVA-EG solution is much faster than that of the PVA-NMP solution. At a lower concentration range, the T'_2 value of PVA-EG gel is lower than that of the PVA-NMP gel. The increase in the chain aggregation in the PVA-EG gel must give rise to reduce the chain mobility of polymer chains, resulting in a lower T'_2 value. The crystallinity obtained from pulsed NMR of the PVA-EG gel increases gradually from 1 to about 9%, while that of PVA-NMP gel has no remarkable change, with a very low value of approximately 1% as the concentration is increased. The only 1% crystallinity in PVA-NMP gel indicates that the primary part of the polymer-rich phase consists mainly of the denser chain entanglements. The quality of the polymer-rich phase is quite different between the PVA-NMP and PVA-EG gels. The discrepancy in the network structure of the PVA gels must be due to the polymer-solvent interaction making the various gelation mechanisms. Because the properties of dilute PVA solutions indicate that the attractive interaction between PVA and NMP is higher than that between PVA and EG. The results in this work let us consider that the gelation of the PVA-NMP solution must occur before the phase separation, resulting in a homogeneous and thinner network structure. On the other hand, the PVA-EG solution first become turbid, and then the gelation occurs to form opaque gels because the poor solubility of the solvent used is more favorable to the intramolecular crystallization for forming the chain-folded crystallites during gelation.

REFERENCES

1. P. D. Hong and K. Miyasaka, *Polymer*, **32**, 3140 (1991).
2. J. Guenet, *Thermoreversible Gelation of Polymers and Biopolymers*, Academic, London, 1992.
3. M. Ohkura, T. Kanaya, and K. Kaji, *Polymer*, **33**, 3689 (1992).
4. M. Ohkura, T. Kanaya, and K. Kaji, *Polymer*, **33**, 5044 (1992).
5. M. Watase and K. Nishinari, *Polym. J.*, **21**, 567 (1989).
6. K. Yamaura, H. Katoh, T. Tanigami, and S. Matsuzawa, *J. Appl. Polym. Sci.*, **34**, 2347 (1987).
7. K. Nishinari and M. Watase, *Polym. J.*, **25**, 463 (1993).
8. P. Cebe and D. Grubb, *J. Mater. Sci.*, **20**, 4465 (1985).
9. V. M. Andreyeva, A. A. Anikeyeva, B. I. Lirova and A. A. Tager, *Vysokomol. Soyed.*, **15**, 1770 (1973).
10. T. J. C. Hosea and S. C. Ng, *Polymer*, **27**, 1864 (1986).
11. W. Stoks, H. Berghmans, P. Moldenaers, and J. Mewis, *Br. Polym. J.*, **20**, 316 (1988).
12. T. Matsuo and H. Inagaki, *Makromol. Chem.*, **53**, 130 (1960).
13. D. Braun and E. Walter, *Colloid Polym. Sci.*, **258**, 376 (1980).
14. O. V. Klenina, V. I. Klenin, and S. Y. Frenkel, *Vysokomol. Soyed.*, **12**, 1277 (1970).
15. M. Watase and K. Nishinari, *Polym. J.*, **21**, 597 (1989).
16. L. H. Spering, *Introduction to Physical Polymer Science*, Wiley, New York, 1986, pp. 78-89.
17. C. A. Finch, *Polyvinyl Alcohol—Developments*, John Wiley, New York, 1992.
18. S. P. Papkov, S. G. Yefimova, M. V. Shablygin, and N. V. Mikhailov, *Vysokomol. Soyed.*, **8**, 1035 (1966).
19. J. G. Powles and J. H. Strange, *Proc. Phys. Soc., London*, **82**, 6 (1963).
20. S. Meiboom and D. Gill, *Rev. Sci. Instrum.*, **29**, 688 (1958).
21. P. Patel, F. Rodriguez and G. Moloney, *J. Appl. Polym. Sci.*, **23**, 2335 (1979).
22. J. E. Eldridge and J. P. Ferry, *J. Phys. Chem.*, **58**, 992 (1954).
23. K. Yamaura, H. Kitahara, and T. Tanigami, *J. Appl. Polym. Sci.*, **64**, 1283 (1997).
24. H. Maeda, T. Kawai, and R. Kashiwagi, *Kobunshi Kagaku*, **13**, 193 (1956).
25. T. Tanigami, K. Murase, K. Yamaura and S. Matsuzawa, *Polymer*, **35**, 2573 (1994).
26. M. Ohkura, T. Kanaya, and K. Kaji, *Polymer*, **33**, 3686 (1992).
27. T. Ikehara, T. Nishi, and T. Hayashi, *Polym. J.*, **28**, 169 (1996).
28. T. Shiga, K. Fukumopi, Y. Hirose, A. Okada, and T. Kurauchi, *J. Polym. Sci., Polym. Phys. Ed.*, **32**, 85 (1994).
29. K. Fukumori, T. Kurauchi, and O. Kamigaito, *Polymer*, **31**, 713 (1990).
30. S. Kaufman, W. P. Slichter and D. D. Davis, *J. Polym. Sci., A-2*, **9**, 829 (1971).
31. H. Tanaka and T. Nishi, *J. Chem. Phys.*, **85**, 6197 (1986).
32. K. Fujimoto and T. Nishi, *Polym. J.*, **3**, 448 (1972).